1 DOE Award Details

DOE Award Number	DE FG02-05ER15725
Name of Recipients	Ram Seshadri, Susannah Scott, and Juergen Eckert University of California, Santa Barbara, CA 93106
Project title	Nanostructured carbide catalysts for the hydrogen economy
Principal Investigator	Ram Seshadri
Co-Principal Investigator	Susannah Scott and Juergen Eckert
Teaming members	None

2 Distribution limitations

This report is furnished with unlimited rights.

3 Executive summary

> *"The second grand challenge in the report centers on design and controlled synthesis of catalyst structures. Fundamental investigations of catalyst structures and the mechanisms of catalytic reactions provide the necessary foundation for the synthesis of improved catalysts."*

The above quote, taken from the executive summary of the Report from the US DOE Basic Energy Sciences Workshop held August 6–8, 2007,[1] places in context the research carried out at the University of California, Santa Barbara, which is reported in this document. The enormous impact of heterogeneous catalysis is exemplified by the Haber process for the synthesis of ammonia, which consumes a few % of the world's energy supply and natural gas, and feeds as many as a third of the world's population. While there have been numerous advances in understanding the process,[2] culminating in the awarding of the Nobel Prize to Gerhard Ertl in 2007, it is interesting to note that the catalysts themselves have changed very little since they were discovered heuristically in the the early part of the 20th century. The thesis of this report is that modern materials chemistry, with all the empirical knowledge of solid state chemistry, combined with cutting edge structural tools, can help develop and better heterogeneous catalysis.

The first part of this report describes research in the area of early transition metal carbides (notably of Mo and W), potentially useful catalysts for water gas shift (WGS) and related reactions of use to the hydrogen economy. Although these carbides have been known to be catalytically useful since the 1970s,[3] further use of these relatively inexpensive materials have been plagued by issues of low surface areas and ill-defined, and often unreactive surfaces, in conjunction with deactivation. We have employed for the first time, a combination of constant-wavelength and time-of-flight neutron scattering, including a total scattering analysis of the latter data, to better understand what happens in these materials, in a manner that for the first time, reveals surface graphitic carbon in these materials in a quantitative manner. Problems of preparation, surface stability, and irreversible reactivity have become manifest in this class of materials that discourage us from pursuing these materials further.

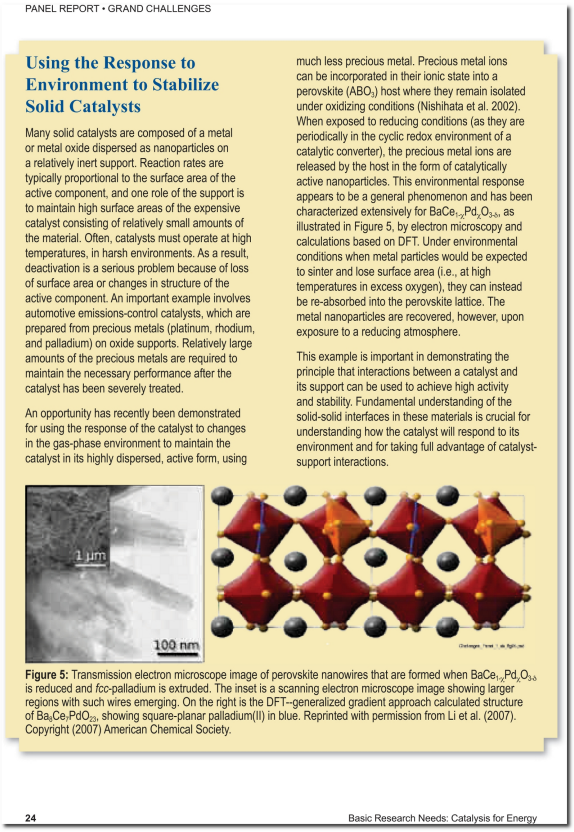

PANEL REPORT • GRAND CHALLENGES

Using the Response to Environment to Stabilize Solid Catalysts

Many solid catalysts are composed of a metal or metal oxide dispersed as nanoparticles on a relatively inert support. Reaction rates are typically proportional to the surface area of the active component, and one role of the support is to maintain high surface areas of the expensive catalyst consisting of relatively small amounts of the material. Often, catalysts must operate at high temperatures, in harsh environments. As a result, deactivation is a serious problem because of loss of surface area or changes in structure of the active component. An important example involves automotive emissions-control catalysts, which are prepared from precious metals (platinum, rhodium, and palladium) on oxide supports. Relatively large amounts of the precious metals are required to maintain the necessary performance after the catalyst has been severely treated.

An opportunity has recently been demonstrated for using the response of the catalyst to changes in the gas-phase environment to maintain the catalyst in its highly dispersed, active form, using much less precious metal. Precious metal ions can be incorporated in their ionic state into a perovskite (ABO_3) host where they remain isolated under oxidizing conditions (Nishihata et al. 2002). When exposed to reducing conditions (as they are periodically in the cyclic redox environment of a catalytic converter), the precious metal ions are released by the host in the form of catalytically active nanoparticles. This environmental response appears to be a general phenomenon and has been characterized extensively for $BaCe_{1-x}Pd_xO_{3-\delta}$, as illustrated in Figure 5, by electron microscopy and calculations based on DFT. Under environmental conditions when metal particles would be expected to sinter and lose surface area (i.e., at high temperatures in excess oxygen), they can instead be re-absorbed into the perovskite lattice. The metal nanoparticles are recovered, however, upon exposure to a reducing atmosphere.

This example is important in demonstrating the principle that interactions between a catalyst and its support can be used to achieve high activity and stability. Fundamental understanding of the solid-solid interfaces in these materials is crucial for understanding how the catalyst will respond to its environment and for taking full advantage of catalyst-support interactions.

Figure 5: Transmission electron microscope image of perovskite nanowires that are formed when $BaCe_{1-x}Pd_xO_{3-\delta}$ is reduced and *fcc*-palladium is extruded. The inset is a scanning electron microscope image showing larger regions with such wires emerging. On the right is the DFT–generalized gradient approach calculated structure of $Ba_8Ce_7PdO_{23}$, showing square-planar palladium(II) in blue. Reprinted with permission from Li et al. (2007). Copyright (2007) American Chemical Society.

24 Basic Research Needs: Catalysis for Energy

Figure 1: One of the highlights in the "Grand Challenges" section of the 2007 Panel Report.[1] The figure describes catalysts that respond to the redox environment, reporting on work done as a part of this DOE grant.

The second, and greater part of this report concerns itself with the role that complex oxide hosts (or noble metal ions and nanoparticles) play in heterogeneous catalysis with specific focus on oxidation reactions. This change in the focus of the research (performed with prior authorization from the program manager) has revealed an untold wealth of information on the complex materials chemistry of ions such as Pd^{2+} which are central to a number of catalytic processes. This part of the research has attracted significant attention, having been highlighted in the DOE report mentioned previously (see figure 1).[1]

It is this second part that we continue to pursue in Santa Barbara, in light of the new scientific insights we have obtained in catalysis by PGM ions, the ways suggested for mitigating PGM use, and finally, the promise of replacing PGMs with the related coinage metals in numerous oxidative processes.

4 Comparison of accomplishments with goals and objectives

In the original proposal, we identified a number of issues that we had hoped to address. Key amongst these were that previous syntheses of metal carbides had pointed to the difficulty of obtaining truly high surface area materials. Thomson showed that "solution-derived" materials

which were nominally high surface area actually contained a great deal of excess carbon, and that amorphous carbon was responsible for most of the surface area.[4] High temperature temperature programmed reduction methods give high surface area materials that are incompletely carburized. The major difficulty was in preparing authentic, stoichiometric high surface area carbides.[4] A second problem with earlier syntheses of metal carbides was the lack of control over the phase produced; low surface area materials tend to be the cubic phase (*e.g.* WC), while high surface area materials (with smaller particle sizes) tended to be the hexagonal phase (*e.g.* W_2C).

Early on in the research, we determined that the characterization of these materials using laboratory X-ray diffraction, even for something as simple as phase determination, is untenable, and to truly understand these materials, neutron diffraction (sensitive to the light element, C, in the structure) is essential. We made use of two facilities to this end: constant wavelength neutrons from the diffractometer BT1 at NIST, Gaithersburg, and time-of-flight neutron scattering data from the NPDF diffractometer at the Lujan Center at Los Alamos National Laboratory. One unforeseen consequence of the reliance on neutron scattering is the relatively long time taken to get things done in this area, particularly in light of the project being new. In conjunction with BET surface area analysis, X-ray photoelectron spectroscopy, and thermogravimetric analysis, neutron diffraction revealed both phase composition and excess carbon content. This work has been described in a detailed publication.[5] We summarize the results of the analysis of different synthesis approaches in Table 1.

A key aspect of the carbides study was the use of differential pair distribution function (PDF) methods to analyze surface carbon in the samples prepared by temperature-programmed reduction. Figure 2 displays results of fitting the WC PDF to the the $P\bar{6}m2$ average structure model, to a real-space length of 10 Å in r. The fit is quite poor. However, the difference curve can be fit to the graphite structure, which refines to $a = 2.4602(1)$ Å and $c = 7.58(5)$ Å. This poorly crystalline graphite, which we believe covers the surface of the WC, is hard to detect using other techniques. The W−W distances in WC are close to the C−C diagonal distances in graphite, allowing a natural templating of graphite on WC. The PDF shows that in WC, the graphite structure is coherent to about 8 Å.

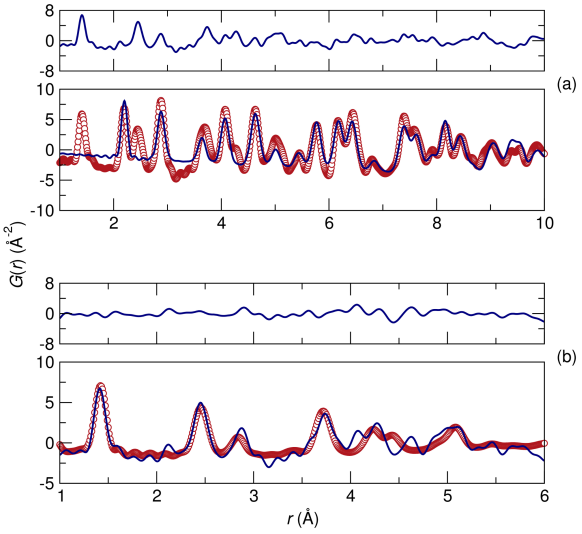

Figure 2: (a) Experimental pair distribution function (circles) and the fit (solid line) for WC. The difference between experiment and fit is displayed at the top of this panel. Note the large peak in the difference PDF near 1.41 Å. (b) Fit of the difference PDF from panel (a) to the structure of hexagonal graphite. The difference between experiment and fit is displayed at the top of this panel.

The carbon-rich mixture of CH_4 and H_2 used to prepare the carbides yields materials with a large amount of excess carbon as seen above in the difference PDF, and as identified by high resolution XPS as both graphitic (g-C-C) and amorphous (a-C-C). These are shown in Figure 3a. Materials prepared with a slow temperature ramp and higher final temperatures have relatively

Table 1: Preparation and characterization of carbide samples. Synthesis conditions are illustrated by precursors (APM = ammonium paramolybdate and APT = ammonium paratungstate), heating rate (H.R.), and carburization temperature, Characterization includes X-ray powder diffraction (XRD), XPS analysis for carbide carbon (C_c), graphitic, amorphous and adventitious carbon (C_g), total carbon (C_t), total oxygen (O_t) and total metal (M_t) content, and BET surface area (S_g) measurement. All the samples are passivated unless otherwise stated. In cases where two heating rate values and two temperatures are displayed, the sample was heated to the first temperature at the first heating rate, and then to the second temperature at the second heating rate. Notes: (1) Samples not exposed to air. (2) Samples subjected to H_2 treatment in 5%H_2/95%N_2 at 600°C for 2 h after carburization.

Precursors	H.R. (°C/min)	Temperature (°C)	XRD	C_c (%)	C_g (%)	C_t (%)	O_t (%)	M_t (%)	S_g (m^2/g)
APM	5	900	Mo_2C	7	74	90	5	5	1
APM	5	700	Mo_2C	11	47	72	14	14	8
APM	5	650	Mo_2C	5	37	55	31	14	18
APM	10,1	300,615	Mo_2C	6	16	29	57	14	5
APM	2	650	Mo_2C	8	40	55	24	21	20
APM	2	650	$Mo_2C^{(1)}$	20	35	63	4	33	52
APM	0.2	650	Mo_2C	13	35	58	20	22	52
MoO_3	2	650	Mo_2C	7	45	57	28	15	22
MoO_3	0.2	650	Mo_2C	12	46	63	20	17	25
APM	10,1	300,650	Mo_2C	15	32	52	14	34	11
APM	10,1	300,650	$Mo_2C^{(2)}$	14	34	55	9	36	9
APT	2	950	WC	6	73	91	4	5	13
APT	2	950	$WC^{(1)}$	3	85	95	2	3	17
APT	2	900	WC	8	52	86	5	9	15
APT	5,1	500,800	WC+W_2C	19	46	74	5	21	24
APT	0.2	900	WC	11	70	89	2	9	24
APT	0.2	900	$WC^{(2)}$	11	69	88	1	11	24
WO_3	0.2	900	WC	7	62	89	4	7	17

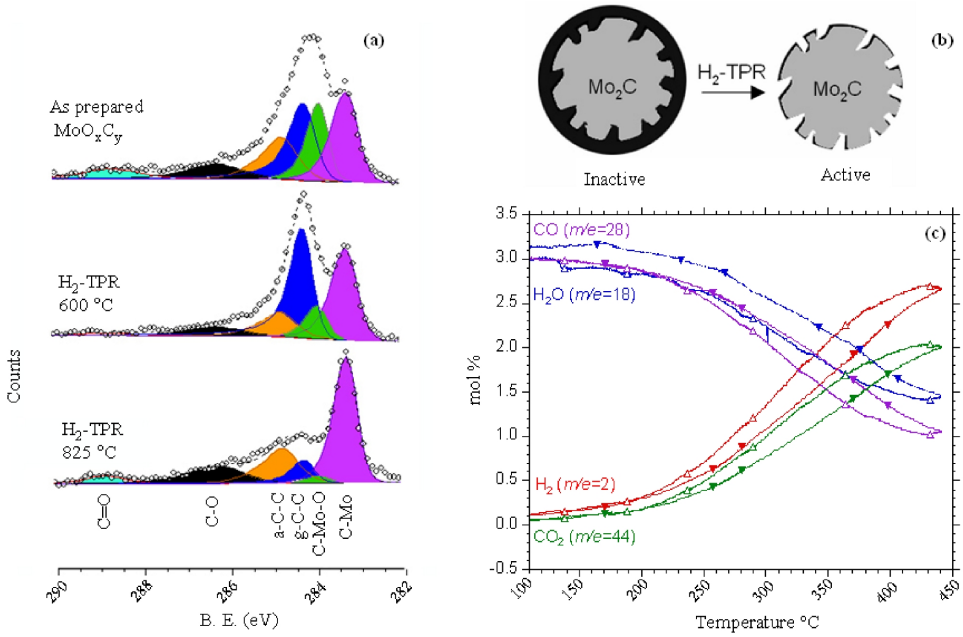

Figure 3: High resolution C 1s XPS (diamonds) of MoO$_x$C$_y$, as-prepared and after TPR in flowing H_2 for 1 h at 600°C and 825°C. The dashed line is the sum of the components. From the left, turquoise (288.76 eV) and black (286.21 eV) components are assigned to carbonates. Orange (284.77 eV) and blue (284.26 eV) components are amorphous and graphitic carbon. The green (283.81 eV) and magenta (283.31 eV) peaks are oxycarbide and carbide phases respectively. (b) Cartoon of catalyst activation by temperature programmed reduction in H_2. (c) Typical temperature-reaction profiles for watergas shift. The reaction was monitored by mass spectrometry using 75 mg catalyst, treated for 1 h at 600°C under flowing H_2 (20 ml/min), in flowing 3%-CO/3-4% H_2O/Ar mixture (20 ml/min) ramped to 450°C at 5°C/min. Up-triangles indicate rising temperature sweeps.

more graphite than amorphous carbon. We can also distinguish between carbide and oxycarbide phases by XPS. BET surface areas are higher for materials with smaller amounts of excess carbon (a-C-C and g-C-C), indicating that the surface area is mostly nanoparticulate Mo_2C rather than finely divided carbon. Activation in H_2 at 600°C removes mostly amorphous carbon [Figure 3(a) and (b)], while graphitic carbon remains on the surface until 825°C. The MoO$_x$C$_y$ materials were evaluated as catalysts for the water-gas shift reaction. As-prepared materials were inactive below 250°C and showed low CO conversion at 450°C, typically less than 25 %. The most significant improvement to the WGS activity was observed after the catalysts were activated by H_2-TPR at 600°C, suggesting that amorphous carbon is mostly responsible for blocking the active sites. CO conversion commenced at 200°C and was typically greater than 90% at 450°C as seen in Figure 3(c). Typical CO conversions between 2 μmol and 5 μmol-CO s^{-1}-g(catalyst)$^{-1}$ were achieved for catalysts activated above 600°C.

Catalysts with higher oxycarbide contents show WGS activity similar to those which are mostly carbides. Increased oxygen content is revealed upon graphite removal without a corresponding increase in oxycarbide content, indicating the presence of molybdenum oxide domains that are not detected by XRD. The role of the graphitic and oxide domains in the WGS activity of Mo_2C requires further study. Our summary conclusion for the carbides work is that given the difficulty

in quickly characterizing the materials in a manner that permits feedback to efforts on preparation and catalytic testing, future work should perhaps be more closely linked to a national neutron facility (Oak Ridge or Los Alamos). Our studies show that the materials are promising, but much more needs doing before their promise is fulfilled.

5 Summary of activities for the entire period

In this section, we describe the new results that emerged from (ongoing) work on the role of platinum group ions (primarily Pd^{2+}) in oxidative heterogeneous catalysis of relevance to processes such as 3-way catalytic converters in automobiles. The genesis of the work was the notion of self-regenerating or "intelligent" catalysts: an idea presented by Nishihata *et al.*[6] In these catalysts, noble metals such as palladium are incorporated in their ionic state in a perovskite oxide host, where they remain under oxidizing conditions. The noble metal ions are released by the host in the form of small particles under reducing conditions, whence they display catalytic activity. Under conditions where the particles would sinter and lose surface area, they are re-absorbed into the perovskite lattice. Catalytic activity is recovered on exposure to a reducing atmosphere. The specific system that the authors used for the demonstration was the perovskite $LaFe_{0.57}Co_{0.38}Pd_{0.05}O_3$, and by performing diffraction experiments at the Pd K-edge, the authors showed that Pd is incorporated on the *B* site of the ABO_3 perovskite structure. In a more recent article, the same group showed that $LaFe_{0.95}Pd_{0.05}O_3$ can be cycled similarly, with reducing conditions giving rise to Pd nanoparticle formation, and oxidizing conditions leading to Pd cation incorporation into the perovskite lattice.[7] Particle sintering and the associated loss of catalytic surface area were significantly reduced when perovskite hosts were employed, in comparison with Pd supported on the more usual Al_2O_3.

We thought it of interest to investigate a system capable of stabilizing Pd^{2+} in relatively large quantities, nearing 10 atom-%, in the *B*-site of the perovskite structure. The perovskite host $Ba^{2+}Ce^{4+}O_3$ was selected on the basis of three crystal chemical principles. First, the large Ce^{+4} ion (radius 0.87 Å in six-coordination) was selected as the host *B* cation so that the *B*-site octahedra could accommodate the large Pd^{2+} ion (radius 0.64 Å in square planar four-coordination and 0.86 Å in six-coordination). The second is the ability of Ba^{2+}, as a consequence of its being large and electropositive, to stabilize high oxidation states on other elements, particularly in the perovskite lattice. The third is that the Ce^{4+}/Ce^{3+} couple could provide this host compound some redox flexibility, if required, that would aid in the substitution.

$BaCeO_3$ turned out to be a wonderful host for Pd in every possible way.[8] Firstly, it admits quite a lot of Pd on the Ce site, up to 10 atom-%. This allows the material to be characterized rather reliably by neutron diffraction as shown in Fig. 4A. Given the high quality (meaning high resolution and high momentum transfer) of the time-of-flight neutron diffraction (NPDF, Los Alamos) it was possible to establish that for each substituted Pd, there was an oxygen vacancy introduced, suggesting that the Ce^{4+} are substituted by Pd^{2+}. XRD performed on the Pd-substituted $BaCeO_3$ samples after successive reduction steps showed that Pd is indeed thrown out of the lattice in reduced form. Two-phase (*fcc*-Pd + $BaCeO_3$) samples could be heated in oxygen or air to recover the substituted perovskite Figure 4B. This suggests that the idea of a system that is responsive to the external redox conditions indeed seems valid. Finally a combination of DFT calculations and pair distributions (Figure 4C) provided a structural model for square-planar Pd^{2+} substituting the octahedral Ce^{4+}

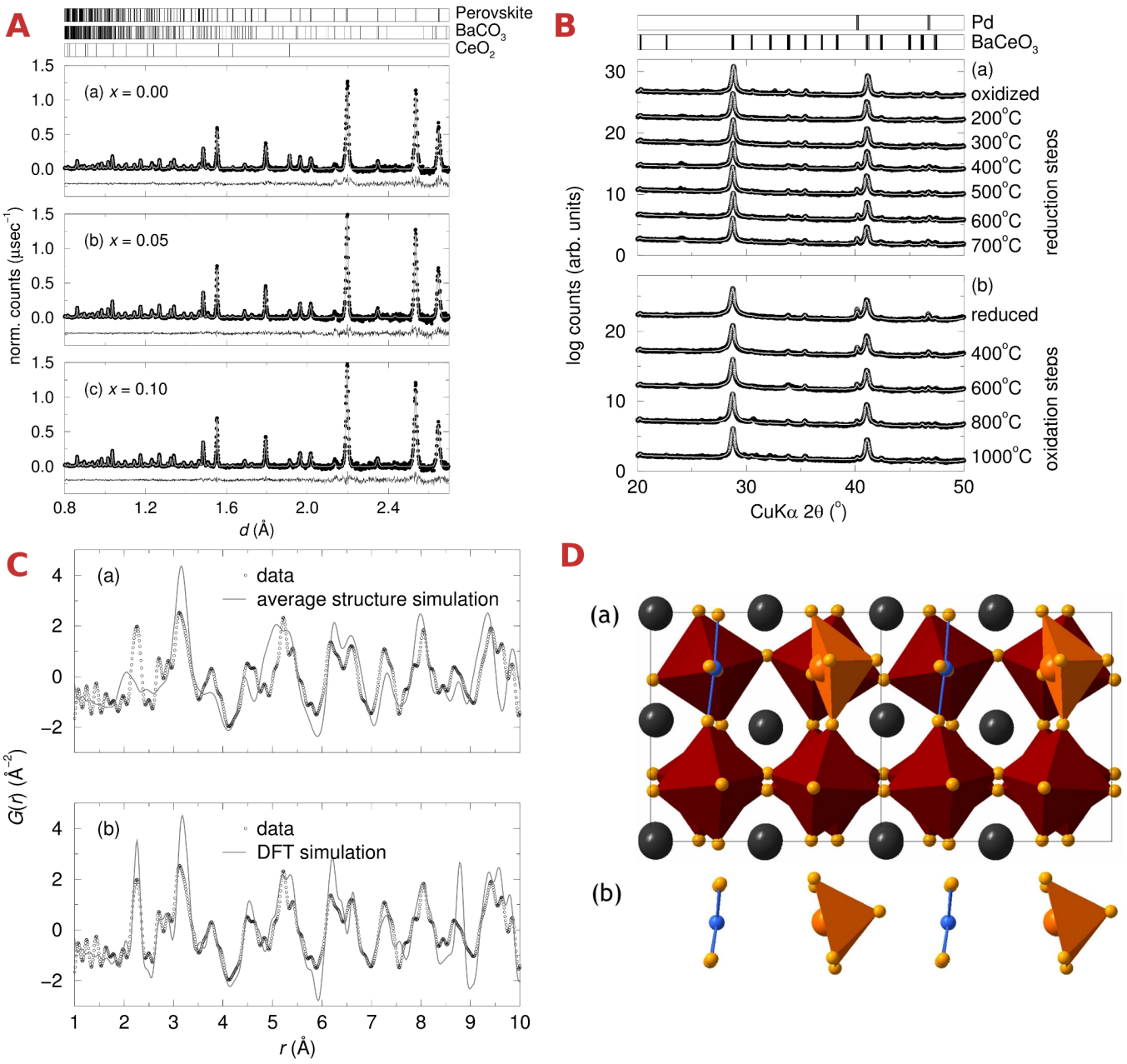

Figure 4: A: Rietveld refinement of the highest-resolution banks of time-of-flight neutron diffraction data acquired on $BaCe_{1-x}Pd_xO_{3-\delta}$ phases with the compositions (a) $x = 0.00$, (b) $x = 0.05$, and (c) $x = 0.10$. For all samples, we found $x \approx \delta$. B: (a) XRD patterns a fully oxidized $BaCe_{1-x}Pd_xO_{3-\delta}$ sample with $x = 0.10$ (topmost trace) and the diffraction patterns obtained on treating different batches of this sample at the different indicated temperatures for 1 h under flowing $5\%H_2/95\%N_2$. The emergence of the principal 111 reflection of *fcc*-Pd near 41° in 2θ with increasing temperature should be noted. (b) This peak starts disseminating when the two-phase perovskite + *fcc*-Pd sample (labeled "reduced") is heated in flowing O_2 at the different indicated temperatures. C: (a) Experimental neutron PDF $G(r)$i of $BaCe_{1-x}Pd_xO_{3-\delta}$ with $x = 0.10$ (data points) compared with the PDF simulated from the average (Rietveld) structure and (b) experimental $G(r)$ compared with the PDF simulation starting from a DFT model of $Ba_8Ce_7PdO_{23}$ shown in panel D. D: (a) Two unit cells of the crystal structure of $Ba_8Ce_7PdO_{23}$, optimized by density functional calculations. (b) The tilting of the CeO_5 square pyramids is clearly seen to result in Pd^{2+} being square planar rather than square pyramidal. This last panel is also seen in Fig. 1.

site in the crystal structure, as depicted in Figure 4D.

Having established that $BaCeO_3$ is a suitable host for the substitution of Pd^{2+} ions, we went on to characterize its efficacy, in both oxidized (phase pure perovskite) and reduced (two-phase *fcc*-Pd nanoparticles and $BeCeO_3$), in oxidative catalysis, using as a test reaction the conversion of CO to CO_2 under oxygen-rich conditions. To our surprise, the catalytic activity of the doped perovskite for CO oxidation in an oxidizing atmosphere appears to be maximized not by the stabilization of Pd nanoparticles or increased dispersion of PdO, but rather by the presence of cationic Pd^{2+} in the perovskite host.[9]

We have since established the importance of Pd^{2+} in other systems as well. For example, the compound $YFeO_3$ is normally stable as a perovskite, although sol-gel preparations indicate the initial (as the sample is heated) formation of a metastable $YFeO_3$ phase with the hexagonal $YAlO_3$ crystal structure. The substitution of Pd^{2+} (again established by neutron diffraction) stabilizes the hexagonal structure of $YFeO_3$.[10] In this system again, redox conditions can be used to tune the single-phase to two-phase (oxide + *fcc*-Pd) transformation. And once again, the most active catalysts are found in the systems with a high content of stabilized Pd^{2+}. In Figure 5, the results of catalysis by the substituted compound $YFe_{0.45}Mn_{0.45}Pd_{0.10}O_3$ in its oxidized (as-prepared), reduced two-phase, and reoxidized forms is displayed and compared with the Pd-free material. The best catalyst (the one with the lowest light-off temperature) is the one that has been reduced and then re-oxidized. The process of reduction/reoxidation restores the original single phase structure and composition, but increases the porosity of the sample. In fact, the relatively low-light off temperatures seen for the samples in Figure 5 are particularly remarkable given that the samples all possess relatively low specific surface areas.

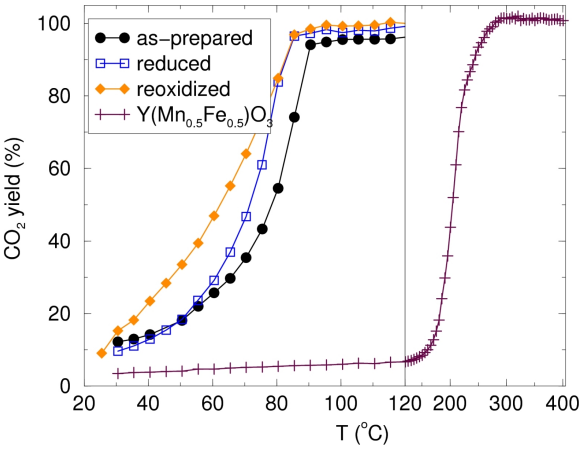

Figure 5: Conversion of CO to CO_2 as a function of temperature. The atmosphere used was 1000 ppm of Co in 9.5%-O_2 in Ar.

The results of Pd^{2+}-substitution in $BaCeO_3$ seem also to be valid for Pt substitution, although a striking difference is that both Pt^{2+} and Pt^{4+} states are found in the substituted compounds. This is the subject of a manuscript that will be written soon. The results obtained in these systems are also informing our current work on other model compounds for Pd^{2+}, as well as isoelectronic Au^{3+}.

Our efforts to address questions relating to the catalytic activity of ions have focused on the preparation of compounds with noble metal ions in well defined coordination sites and oxidation states. One such compound, La_2BaPdO_5, the structure of which is shown in Figure 6a, contains $Pd^{2+}O_4$ square planes in analogy to the coordination environment of Pd in substituted $BaCeO_3$. The highly electropositive lathanum and barium cations are very effective at stabilizing the Pd^{2+} oxidation state, and drive the highly localized bonding between Pd and O observed in the Maximum Entropy reconstruction of the electron density in the unit cell (Figure 6b). The exceptional stability of La_2BaPdO_5, evidenced by TGA, suggests the presence of electropositive cations as criteria for

stabilizing oxophobic PGMs in oxide hosts. While PdO is typically reduced in air ca. 750° C, La_2BaPdO_5 is stable to nearly 1100° C in inert atmosphere (N_2), and is not reduced in 5 % H_2 until nearly 600° C (Figure 6c). When supported on a binary oxide such as CeO_2, PdO is reduced below 100° C. The robustness of this model provides isolated and immobilized Pd^{2+} ions that retain their coordination and oxidation state throughout a test reaction.

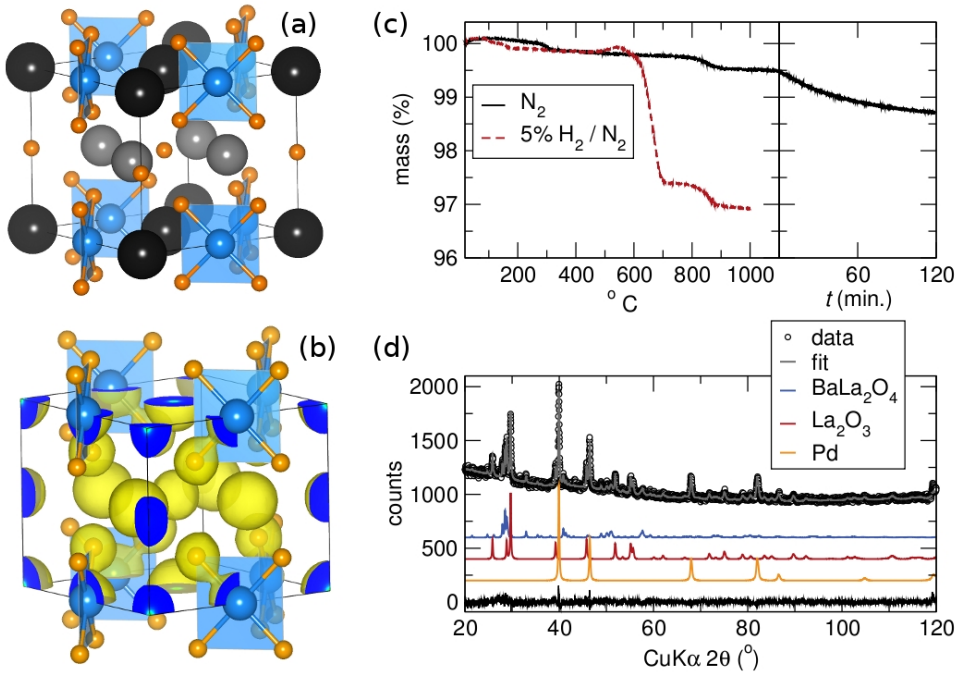

Figure 6: La_2BaPdO_5: (a) Unit cell depiction: Pd (blue), Ba (black), La (gray), O (orange). (b) Charge density isosurfaces as determined by maximum entropy pattern fitting of sychrotron diffraction data, indicating localized (covalent) bonding between O and Pd. (c) The extraordinary stability of this model compound is demonstrated by thermogravimetric analysis in N_2 and 5 % H_2. (d) Rietveld refinement of decomposition products from a sample of La_2BaPdO_5 reduced in 5 % H_2.

One important difference between the model and $BaCe_{1-x}Pd_xO_{3-\delta}$ is the absence of vacancies on the oxide sublattice in La_2BaPdO_5. Oxygen vacancies are believed to facilitate oxidative catalysis through the labilization of oxide from the bulk in a Mars van Krevelen type mechanism. However, La_2BaPdO_5 is nonetheless a very good CO oxidation catalyst. Indeed, in comparison to a reduced (decomposed) sample of La_2BaPdO_5 that contained *fcc*-Pd metal, La_2O_3, and $BaLa_2O_4$ (Figure 6d), the Pd^{2+} model displays a light off temperature about 40° C lower than the reduced multi-phase material. This finding provides further support to the belief that precious metal ions play an important role in catalytic oxidation.

6 Products and publications

In the order that they appeared, the following papers have been published as a result of this support:

1. X. Ouyang, J. Li, R. Seshadri, and S. L. Scott, A Highly active and reusable catalyst for Suzuki

coupling: $BaCe_{1-x}Pd_xO_{3-x}$ ($0 < x \leq 0.1$), Catalysis of Organic Reactions: 22nd Conference, CRC Press, December 2008.

2. J. Li, U. G. Singh, J. W. Bennett, K. Page, J. Weaver, J.-P. Zhang, Th. Proffen, A. M. Rappe, S. Scott, and R. Seshadri, $BaCe_{1-x}Pd_xO_{3-\delta}$ ($0 \leq x \leq 0.1$): Redox controlled ingress and egress of palladium in a perovskite, *Chem. Mater.* **19** (2007) 1418-1426. [**doi**]

3. U. G. Singh, J. Li, J. W. Bennett, A. M. Rappe, R. Seshadri, and S. L. Scott, A Pd-doped Perovskite Catalyst, $BaCe_{1-x}Pd_xO_3$, for CO Oxidation, *J. Catal.* **249** (2007) 349-358. [**doi**]

4. J. Li, U. G. Singh, T. D. Schladt, J. K. Stalick, S. L. Scott, and R. Seshadri, Hexagonal $YFe_{1-x}Pd_xO_3$: Non-perovskite host compounds for Pd^{2+} and their catalytic activity for CO oxidation. *Chem. Mater.* **20** (2008) 6567–6576. [**doi**]

5. K. Page, J. Li, R. Savinelli, H. N. Szumila, J. Zhang, J. K. Stalick, Th. Proffen, S. L. Scott, and R. Seshadri, Reciprocal space and real-space neutron investigation of nanostructured Mo_2C and WC. *Solid State Sci.* **10** (2008) 1499–1510. [**doi**]

References

[1] Basic Research Needs: Catalysis for Energy, Report from the U.S. Department of Energy, Office of Basic Energy Sciences Workshop August 6–8, 2007, in Bethesda, Maryland.

[2] G. Ertl, Reactions at surfaces: From atoms to complexity, Nobel Lecture, December 8, 2007 (copyright The Nobel Foundation).

[3] R. B. Levy and M. Boudart, Platinum-like behavior of tungsten carbide in surface catalysis, *Science* **181** (1973) 547–549.

[4] D. C. LaMont, A. J. Gilligan, A. R. S. Darujati, A. S. Chellappa, and W. J. Thomson, The effect of Mo_2C synthesis and pretreatment on catalytic stability in oxidative reforming environments, *Appl. Catal. A: Gen.* **255** (2003) 239–253.

[5] K. Page, J. Li, R. Savinelli, H. N. Szumila, J. Zhang, J. K. Stalick, Th. Proffen, S. L. Scott, and R. Seshadri, Reciprocal space and real-space neutron investigation of nanostructured Mo_2C and WC, *Solid State Sci.* **10** (2008) 1499–1510.

[6] Y. Nishihata, J. Mizuki, T. Akao, H. Tanaka, M. Uenishi, M. Kimura, T. Okamoto, and N. Hamada, Self-regeneration of a Pd-perovskite catalyst for automotive emissions control, *Nature* **418** (2002) 164–167.

[7] H. Tanaka, I. Tan, M. Uenishi, M. Taniguchi, M. Kimura, Y. Nishihata, and J. Mizuki, $LaFePdO_3$ perovskite automotive catalyst having a self-regenerative function, *J. Alloys Compd.* **408–412** (2006) 1071–1077.

[8] U. G. Singh, J. Li, J. W. Bennett, A. M. Rappe, R. Seshadri, and S. L. Scott, A Pd-doped Perovskite Catalyst, $BaCe_{1-x}Pd_xO_3$, for CO Oxidation, *J. Catal.* **249** (2007) 349-358.

[9] U. G. Singh, J. Li, J. W. Bennett, A. M. Rappe, R. Seshadri, and S. L. Scott, A Pd-doped Perovskite Catalyst, $BaCe_{1-x}Pd_xO_3$, for CO Oxidation, *J. Catal.* **249** (2007) 349-358.

[10] J. Li, U. G. Singh, T. D. Schladt, J. K. Stalick, S. L. Scott, and R. Seshadri, Hexagonal $YFe_{1-x}Pd_xO_3$: Non-perovskite host compounds for Pd^{2+} and their catalytic activity for CO oxidation. *Chem. Mater.* **20** (2008) 6567–6576.